NeuroImage 136 (2016) 1–9

Contents lists available at ScienceDirect

NeuroImage

journal homepage: www.elsevier.com/locate/ynimg

Prediction of brain maturity in infants using machine-learning algorithms

Christopher D. Smyser [a,b,c,*], Nico U.F. Dosenbach [a], Tara A. Smyser [d], Abraham Z. Snyder [a,c], Cynthia E. Rogers [d], Terrie E. Inder [e], Bradley L. Schlaggar [a,b,c,d,f], Jeffrey J. Neil [g]

[a] Department of Neurology, Washington University School of Medicine, 660 South Euclid Avenue, Saint Louis, MO 63110-1093, USA
[b] Department of Pediatrics, Washington University School of Medicine, 660 South Euclid Avenue, Saint Louis, MO 63110-1093, USA
[c] Mallinckrodt Institute of Radiology, Washington University School of Medicine, 660 South Euclid Avenue, Saint Louis, MO 63110-1093, USA
[d] Department of Psychiatry, Washington University School of Medicine, 660 South Euclid Avenue, Saint Louis, MO 63110-1093, USA
[e] Department of Pediatric Newborn Medicine, Brigham and Women's Hospital, 75 Francis Street, Boston, MA 02115, USA
[f] Department of Neurobiology, Washington University School of Medicine, 660 South Euclid Avenue, Saint Louis, MO 63110-1093, USA
[g] Department of Neurology, Boston Children's Hospital, 333 Longwood Avenue, Boston, MA 02115, USA

ARTICLE INFO

Article history:
Received 22 June 2015
Revised 5 May 2016
Accepted 8 May 2016
Available online 11 May 2016

Keywords:
Developmental neuroimaging
Functional MRI
Infant
Prematurity
Multivariate pattern analysis

ABSTRACT

Recent resting-state functional MRI investigations have demonstrated that much of the large-scale functional network architecture supporting motor, sensory and cognitive functions in older pediatric and adult populations is present in term- and prematurely-born infants. Application of new analytical approaches can help translate the improved understanding of early functional connectivity provided through these studies into predictive models of neurodevelopmental outcome. One approach to achieving this goal is multivariate pattern analysis, a machine-learning, pattern classification approach well-suited for high-dimensional neuroimaging data. It has previously been adapted to predict brain maturity in children and adolescents using structural and resting state-functional MRI data. In this study, we evaluated resting state-functional MRI data from 50 preterm-born infants (born at 23–29 weeks of gestation and without moderate–severe brain injury) scanned at term equivalent postmenstrual age compared with data from 50 term-born control infants studied within the first week of life. Using 214 regions of interest, binary support vector machines distinguished term from preterm infants with 84% accuracy ($p < 0.0001$). Inter- and intra-hemispheric connections throughout the brain were important for group categorization, indicating that widespread changes in the brain's functional network architecture associated with preterm birth are detectable by term equivalent age. Support vector regression enabled quantitative estimation of birth gestational age in single subjects using only term equivalent resting state-functional MRI data, indicating that the present approach is sensitive to the degree of disruption of brain development associated with preterm birth (using gestational age as a surrogate for the extent of disruption). This suggests that support vector regression may provide a means for predicting neurodevelopmental outcome in individual infants.

Introduction

Resting state-functional magnetic resonance imaging (rs-fMRI) has been increasingly applied to study functional network development in infants (Doria et al., 2010; Fransson et al., 2009, 2007; Lin et al., 2008; Smyser et al., 2010). Despite differences in study populations and analysis methods, multiple studies have now consistently shown that infants demonstrate resting state networks (RSNs) similar to those which compose the canonical, large-scale functional network architecture supporting motor, sensory and cognitive functions in older pediatric and adult populations. During the neonatal period, these RSNs demonstrate differing rates of development which reflect known patterns of cortical maturation based upon histological investigations (Gao et al., 2014; Smyser et al., 2016). Recently, quantitative methodology revealed group-level differences in intrinsic brain activity within

Abbreviations: rs-fMRI, resting state-functional magnetic resonance imaging; RSN, resting state network; PMA, postmenstrual age; SVM, support vector machine; MVPA, multivariate pattern analysis; SVR, support vector regression; GA, gestational age; NICU, neonatal intensive care unit; EPI, echo-planar-image; BOLD, blood oxygen level dependent; ROI, region of interest; LOOCV, leave-one-out-cross-validation; MNI, Montreal Neurological Institute.

* Corresponding author at: 660 South Euclid Avenue, Campus Box 8111, Saint Louis, MO 63110-1093, USA.
E-mail addresses: smyserc@neuro.wustl.edu (C.D. Smyser), dosenbachn@neuro.wustl.edu (N.U.F. Dosenbach), smysert@psychiatry.wustl.edu (T.A. Smyser), avi@npg.wustl.edu (A.Z. Snyder), rogersc@psychiatry.wustl.edu (C.E. Rogers), tinder@partners.org (T.E. Inder), schlaggarb@neuro.wustl.edu (B.L. Schlaggar), jeffrey.neil@childrens.harvard.edu (J.J. Neil).

http://dx.doi.org/10.1016/j.neuroimage.2016.05.029
1053-8119/

these RSNs during the neonatal period due to prematurity (Smyser et al., 2016). These findings suggest that functional network development is altered during the critical period of brain development prior to term equivalent postmenstrual age (PMA; *i.e.*, 38–40 weeks) during which significant brain growth and folding are typically occurring. However, the role of alterations in these RSNs in determining neurodevelopmental outcomes remains incompletely understood, as are the clinical factors associated with these changes. Application of novel analytical approaches is an important step in translating our improved understanding of early functional connectivity into predictive models of neurodevelopmental outcome applicable in individuals.

Support vector machine (SVM)-multivariate pattern analysis (MVPA) is a machine-learning, pattern classification method that can be used to investigate complex patterns in high-dimensional neuroimaging data (Dosenbach et al., 2010; Pereira et al., 2009; Scholkopf and Smola, 2002; Smola, 2004). This technique is well-suited to accommodate and analyze large, multi-dimensional neuroimaging data sets, identifying data-driven decision boundaries which can be used to maximally separate populations of interest while identifying features within these data most important for discriminating between groups. This brain-wide approach provides a conceptual shift for the functional neuroimaging field, contextualizing results obtained through investigations focused on specific areas of the brain, while increasing the likelihood of identifying population differences by investigating much larger numbers of brain regions in comparison to currently employed univariate models. It has been employed to investigate brain-wide patterns of functional and structural connectivity, creating classifiers which differentiate groups with high accuracy and identifying connections critical for distinguishing clinical populations based upon age and diagnosis such as Alzheimer's disease, autism spectrum disorder, addiction, schizophrenia and obsessive–compulsive disorder (Brown et al., 2012; Ecker et al., 2010; Erus et al., 2014; Fair et al., 2012; Franke et al., 2012; Li et al., 2014; Magnin et al., 2009; Meier et al., 2012; Pariyadath et al., 2014; Robinson et al., 2010; Rosa et al., 2015; Shen et al., 2010; Vergun et al., 2013). Importantly, these methods can be extended to SVM regression (SVR) to enable quantitative predictions in individuals for variables such as chronological age or developmental status (Pereira et al., 2009; Smola, 2004). Recently, investigators have used this technique to develop predictive models of brain maturity in individual subjects across pediatric and adult populations (Franke et al., 2012; Satterthwaite et al., 2014; Vergun et al., 2013).

Here, we apply SVM methodology to infant rs-fMRI data. We studied 50 preterm infants born at 23–29 weeks of gestation and without moderate–severe injury on structural imaging at term equivalent PMA (hereafter referred to as "preterm-born infants") and 50 healthy, term-born control infants (hereafter referred to as "term-born infants"). Low motion rs-fMRI data were available for all subjects. Using rs-fMRI correlation matrices constructed using 214 cortical and subcortical gray matter regions of interest (ROIs) which delineated the functional connections (*i.e.*, features) between each ROI pair, binary SVMs were used to categorize infants as term-born or preterm-born at the group level based upon birth gestational age (GA). To investigate the effects of prematurity on network architecture, the SVM classification vectors were extracted to identify the functional connections between regions critical for accurate group classification, providing an indication of which connections are altered in preterm infants at term equivalent PMA. We also evaluated the effects of potential modifiers on SVM results, including sex, race, PMA at scan, head size and motion parameters. To explore the potential utility of rs-fMRI data to predict neurodevelopmental outcome, the data were analyzed using SVR. Using GA at birth as an indicator of the degree of disruption of normal brain development in preterm infants, we developed models to estimate an infant's GA at birth based upon rs-fMRI data collected at term equivalent PMA. Such an SVR-derived estimate could provide a measure with which to predict neurodevelopmental outcome in individual infants from single data sets in this high-risk population.

Materials and methods

Subjects

Preterm infants born prior to 30 weeks of gestation were prospectively recruited from the St. Louis Children's Hospital Neonatal Intensive Care Unit (NICU). Term-born infants were recruited from the Barnes-Jewish Hospital Newborn Nursery. All term-born infants had no history of *in utero* illicit substance exposure and no evidence of acidosis (pH > 7.20) on umbilical cord or arterial blood gas assessments during the first hour of life. In both groups, infants were excluded if found to have chromosomal abnormality or suspected or proven congenital infection (*e.g.*, HIV, sepsis, toxoplasmosis, rubella, cytomegalovirus and herpes simplex virus). Parental informed consent was obtained for each subject prior to participation in the study.

Anatomic MR images and cranial ultrasounds (if available) for all subjects were reviewed by a neuroradiologist (J.S.) and pediatric neurologist (C.S.). Infants were excluded from the study if abnormalities, including grade III–IV intraventricular hemorrhage, cystic periventricular leukomalacia, moderate–severe cerebellar hemorrhage or lesions in the deep or cortical gray matter, were detected. All aspects of the study were approved by the Washington University School of Medicine's Human Studies Committee.

The preterm-born group was comprised of 50 infants with a mean GA of 26 weeks (±2, range 23–29 weeks). Twenty-four infants were female and 23 were African-American. The preterm-born infants were scanned at a mean PMA of 38 weeks (±1, range 36–41 weeks). The timing of scan acquisition for these subjects was determined by clinical status and medical course. Additional demographic and clinical information for the preterm-born cohort is provided in Table 1.

The term-born group included 50 infants. For this group, the mean GA at birth was 39 weeks (±1, range 37–41 weeks) with a mean PMA at scan of 39 weeks (±1, range 37–41 weeks). Twenty-three infants were female and 31 were African-American.

Data acquisition

Term-born infants underwent MRI within the first four days of life. Preterm-born infants underwent MRI at term equivalent PMA. Infants were imaged without sedation during natural sleep or while resting quietly with eyes closed (Mathur et al., 2008). Noise protection during scanning was provided by ear muffs (Natus Medical, Foster City, CA). Arterial oxygen saturation and heart rate were continuously monitored throughout acquisition. A NICU staff member was present in the scanner room throughout the study.

Imaging was performed using a Siemens Trio 3T scanner (Erlangen, Germany) and an infant-specific, quadrature head coil (Advanced Imaging Research, Cleveland, OH). Structural images were collected using a T2-weighted sequence (TR 8600 ms; echo time 161 ms; voxel size $1 \times 1 \times 1$ mm^3; echo train length 17). rs-fMRI data were collected utilizing a gradient echo, echo-planar-image (EPI) sequence sensitized to T2* BOLD contrast (TR 2910 ms; echo time 28 ms; voxel size $2.4 \times 2.4 \times 2.4$ mm^3; flip angle 90°). Whole brain coverage was obtained with 44 contiguous slices. Each rs-fMRI run included 200 volumes (frames). A minimum of one run (9.7 min) was obtained in each infant. Additional runs were acquired in a subset of participants depending upon subject tolerance.

Data analysis

rs-fMRI preprocessing

rs-fMRI data were preprocessed as previously described (Smyser et al., 2016). These procedures were implemented using the local 4dfp suite of tools (ftp://imaging.wustl.edu/pub/raichlab/4dfp_tools/). Briefly, this included correction for asynchronous slice timing and rigid body correction of head movement. In addition, EPI distortions in the BOLD

Table 1
Demographic information for term and preterm subjects.

Clinical variable	Number of preterm infants (n = 50)	Number of term infants (n = 50)	p value
Gestational age at birth (weeks) — mean (SD)	26 (2)	39 (1)	<0.0001[a]
Female — n (%)	24 (48)	23 (46)	0.841[b]
African-American — n (%)	23 (46)	31 (62)	0.224[b]
Postmenstrual age at scan (weeks) — mean (SD)	38 (1)	39 (1)	
Birth weight (g) — mean (SD)	896 (242)		
Multiple gestation — n (%)	21 (42)		
Intrauterine growth restriction — n (%)	3 (6)		
Antenatal steroids — n (%)	44 (88)		
Inotropic support — n (%)	15 (30)		
Postnatal steroids — n (%)	12 (24)		
Positive pressure ventilation — n (%)	41 (82)		
Total positive pressure days — mean (SD)	11 (14)		
Total ventilator days — mean (SD)	13 (22)		
Total parenteral nutrition (days) — mean (SD)	27 (23)		
Patent ductus arteriosus treated medically — n (%)	24 (48)		

[a] Result from two-sample, two-tailed *t*-test.
[b] Result from chi-square test.

data were corrected using the FUGUE module in FSL (Jenkinson et al., 2012). Individual magnetization field maps were not acquired in all subjects. Therefore, magnetization inhomogeneity-related distortions were corrected using a mean field map technique (Gholipour et al., 2008). T2-weighted images were aligned with a postmenstrual age-specific infant target to account for differences in cerebral volume and shape between infants and adults (Smyser et al., 2010). Affine transform to register the rs-fMRI first frame with the corrected T2-weighted image was then calculated. The volumetric time series were then realigned to the representative adult template in Talairach atlas space used at the Washington University Neuroimaging Laboratory, combining motion correction and atlas transformation in a single re-sampling step, producing $3 \times 3 \times 3$ mm^3 voxels.

Additional preprocessing to reduce artifact in preparation for rs-fMRI analyses included removal by regression of nuisance waveforms derived from rigid body motion correction, regions in cerebrospinal fluid and white matter, plus the global signal averaged over the whole brain (Power et al., 2014, 2015). The data were passed through a temporal low pass filter retaining frequencies below 0.08 Hz and spatially smoothed (6 mm full-width at half-maximum in each direction). We employed rigorous frame censoring criteria: frames corrupted by motion were identified by analysis of the fully preprocessed volumetric time series (Power et al., 2014). Frames affected by sudden change in head position (framewise displacement ≥0.5 mm) or root mean squared BOLD signal intensity change (DVARS ≥0.5%) were excluded from the rs-fMRI computations ("scrubbing"). A minimum of 5 min of fMRI data, excluding motion censored frames, was required for subject inclusion, with all subjects not meeting this criterion excluded.

To control for potential biases attributable to differing amounts of data included per group, for all term and preterm subjects only the first 100 frames (corresponding to ~5 min) of low-motion rs-fMRI data passing the motion scrubbing parameters delineated above were included in the analysis, with exclusion of all other data for each subject. This procedure ensured that an identical amount of data was analyzed both for each subject and each cohort.

ROI selection

Following transformation of the infant data to adult Talairach atlas space, ROIs (n = 264) in cortical and subcortical gray matter regions were selected using coordinates identified from task data and cortical functional areal parcellations obtained in typical adults (Cohen et al., 2008; Power et al., 2011). Each ROI was a 10-mm diameter sphere centered upon Talairach atlas coordinates. To identify ROIs erroneously placed outside gray matter regions, two procedures were undertaken. First, mean values were measured within each ROI from each subject's Talairach atlas space-registered BOLD data. Second, three viewers (authors C.S. and T.S. and collaborator J.K.) independently visually inspected each ROI location overlaid on the T2-weighted infant data transformed into Talairach atlas space. Using these procedures, 50 ROIs were identified to either have mean BOLD measures outside the typical range for gray matter or be located outside the whole brain mask and/or anticipated gray matter regions. When the initial assessments were discrepant (<2% of all ROIs), a consensus was reached among the viewers. These ROIs were subsequently removed, leaving 214 remaining ROIs (Fig. 1). Pairwise Pearson correlation values were generated between the BOLD time series for each ROI with every other ROI generating a square rs-fMRI matrix (214 × 214) for each subject. This approach resulted in 22,791 interregional correlations for each subject. Correlation coefficients were then Fisher z-transformed to ensure normality (Jenkins and Watts, 1968). ROI assignments by network in adults (Power et al., 2011) and centers for all ROIs are reported in Supplemental Tables 1 and 2.

Support vector machine analyses

The SVM methods employed were adapted from the existing literature (Ben-Hur et al., 2008; Kohavi, 1995; Pereira et al., 2009; Smola, 2004). These procedures included *t*-test filtering to include only reliably different features, linear kernel separation and soft margin separation.

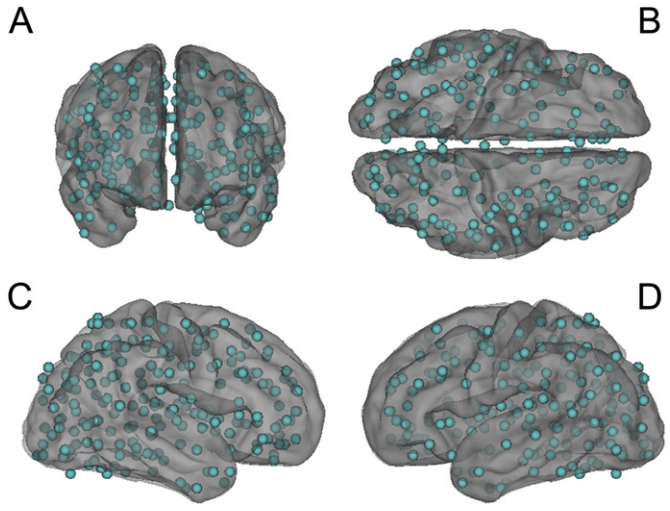

Fig. 1. Cortical, subcortical and cerebellar regions of interest (ROIs) used in the present analyses. Two hundred and fourteen gray matter ROIs assigned to 13 resting state networks in adults (Power et al., 2011) were selected based upon anatomic location from an ROI set derived from task data and cortical functional areal parcellations in adults. Anterior (A), dorsal (B), right (C) and left (D) lateral views presented. ROIs are overlaid on a neonate-specific atlas image.

Leave-one-out-cross-validation (LOOCV), which is widely used in machine learning approaches and provides a good estimate of each classifier's or predictor's true accuracy, was used to estimate group classification (SVM) and prediction (SVR) accuracies. In LOOCV, each sample is designated as the test sample once. Subsequently, there are as many folds (*i.e.*, rounds of cross-validation) as samples. All SVM computations were conducted using the Spider MATLAB Machine-Learning Toolbox (http://www.kyb.tuebingen.mpg.de/de/bs/people/spider) implemented in MATLAB version 7.8.0 (R2009a; The MathWorks, Natick, MA). The MATLAB Bioinformatics, Curve-Fitting and Statistics Toolboxes and in-house MATLAB code were also utilized.

For each subject, each pairwise z(r) value (*i.e.*, functional connection) was defined as a feature for use by the classifier. For SVM classification, 22,791 two-sided *t*-tests (assuming unequal variance) were performed in each LOOCV fold. Within each fold, features were ranked by absolute *t*-score in descending order (the subject tested by the trained machine was also left out of the *t*-test filtering for that LOOCV). To improve computation speed and performance and following well-established, standard procedures, only the top 180 features that most reliably differed between groups were retained for classification. Based upon inspection of LOOCV results across higher thresholds, this feature-filtering number provides maximum relative discriminatory power while avoiding circularity bias (Dosenbach et al., 2010).

For SVR prediction, the correlation of each of the 22,791 features with the independent training variable (*i.e.*, GA) was computed on each LOOCV fold. For each fold, features were similarly ranked by the absolute value of the correlation coefficients with the training variable in descending order (again with the subject tested by the trained machine left out of the *t*-test filtering for that LOOCV), with the top 180 similarly retained for prediction (Dosenbach et al., 2010).

On every fold of the LOOCV for both approaches, feature combinations may be different because every fold differs slightly. Features that were retained across folds were termed consensus features. Those contained in 100% of the folds (*i.e.*, 100% consensus features) were used to construct visualizations of ROIs and functional connections using CARET version 5.65 (Van Essen et al., 2001). ROI weights were computed by summing across all functional connections for each ROI. Extracted feature weights were averaged over all folds.

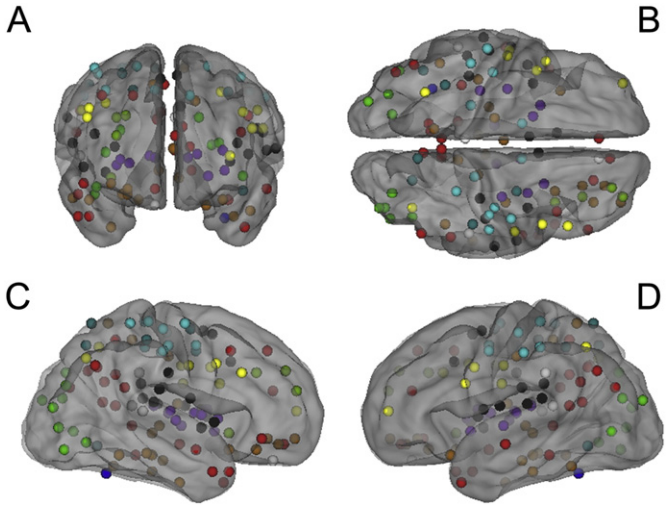

Fig. 2. Regions of interest (ROIs) important for differentiating term-born and preterm-born subjects using binary SVMs. Node colors represent assignment to resting state networks in adults (Power et al., 2011). Black = cingulo-opercular, red = default mode, yellow = frontoparietal, dark blue = cerebellum, green = visual, cyan = somatomotor, yellow-green = lateral somatomotor, dark cyan = dorsal attention, purple = subcortical, gray = ventral attention, brown = unnamed 1, and white = unnamed 2. Note distribution of ROIs throughout the brain and across multiple networks. Anterior (A), dorsal (B), right (C) and left (D) lateral views presented. ROIs are overlaid on a neonate-specific atlas image.

An SVM classifier was initially constructed based upon subject GA (term-born *versus* preterm-born). To investigate whether the accuracy of the term-born *versus* preterm-born categorization was driven by differences between groups in sex, race, PMA at scan, atlas scaling and motion parameters, additional SVM classifiers were created. For binary variables, SVMs were constructed using only data acquired from subjects within the term and preterm groups restricted to a single demographic category (*e.g.*, only male subjects). For continuous variables (*e.g.*, motion parameters), the 50 term subjects were divided into two equal groups of 25 subjects with values above and below the median measure for the variable of interest. Comparable analyses were also performed using only data from preterm-born infants. For SVR prediction, investigated training variables included GA, framewise displacement and DVARS values.

Reported SVM results include classifier accuracy, sensitivity, specificity and p-values for binomial probabilities. Sensitivity is defined as the percent of correctly classified term-born infants within all term-born infants. Specificity is defined as the percent of correctly classified preterm-born infants within all preterm-born infants (*i.e.*, those correctly identified as not term-born). The p-values represent the probability of observing the reported accuracy (number of correct classification trials) by chance based upon the binomial distribution for the given sample size.

Results

SVM term vs preterm classification

Using rs-fMRI matrices of functional connections between ROIs, binary SVMs reliably classified term-born *versus* preterm-born infants studied at term equivalent PMA with 84% accuracy, 90% sensitivity and 78% specificity ($p < 0.00001$). The ROIs that formed the functional connections which contributed to accurate group classification are located throughout the brain and are illustrated in Fig. 2 (also see Supplemental Fig. 1). In adults, these ROIs would populate 13 of the 14 networks from Power et al. (2011), most frequently including ROIs from the default mode, cingulo-opercular, somatomotor, visual, dorsal attention and salience networks. Removal of the ten ROIs that had the functional connections with the greatest classification power did not substantively affect the binary SVM's ability to differentiate preterm-born and term-born subjects (75% accuracy, 80% sensitivity, 70% specificity, $p < 0.00001$).

In these analyses, 126 consensus features for group differentiation were identified. Fig. 3 illustrates these consensus functional connections scaled by the extracted weighting assigned to each feature (green connections stronger in term-born infants, orange stronger in preterm-born infants). Included are intra- and inter-hemispheric connections located throughout the brain. The predominance of both within and between network consensus features was greater in term-born infants (69% *versus* 31%). Between network features contributed more frequently to accurate classification than within network features (82% *versus* 18%). Contributing within network features most prominently included the default mode, cingulo-opercular, dorsal attention and visual networks. The mean Euclidean distance in stereotaxic space for term contributing features (green connections) was 51.8 ± 30.0 mm. For preterm contributing features (orange connections), the mean distance was 51.6 ± 27.8 mm. These distance measures were not different between groups ($p = 0.98$). In addition, feature distance did not correlate with weighting ($p = 0.12$).

Despite smaller subject numbers, SVM classifiers including only data from term and preterm subjects categorized based upon binary variables (*e.g.*, only male subjects) demonstrated classification ability consistent with the larger group analysis (Table 2). Features important for group differentiation were generally similar across classifiers and consistent with the classifier generated using all data. In contrast, binary SVMs created using only data from term-born infants divided according

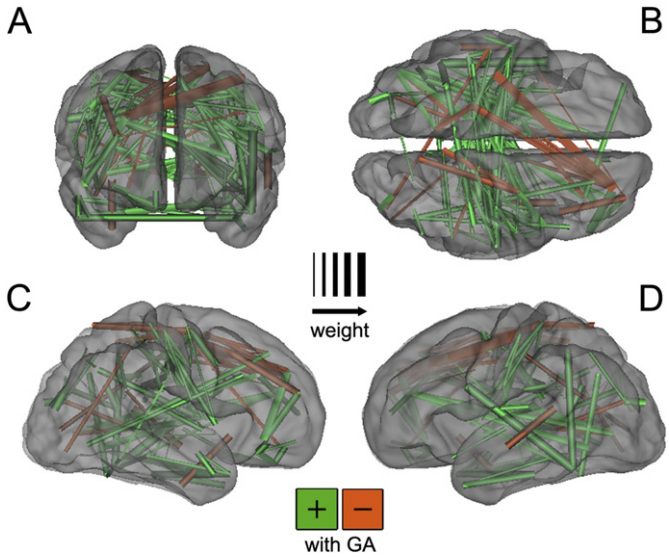

Fig. 3. Consensus features important for differentiating term-born and preterm-born subjects using binary SVMs. One hundred and twenty-six consensus features (100% overlap across all cross-validation folds) distinguished term-born and preterm-born subjects with 84% accuracy. Features are scaled by their weights, which denote their relative importance in group differentiation. Green lines denote functional connections stronger in term-born subjects, whereas orange lines denote functional connections contributing to preterm classification. Note distribution of features throughout the brain. Anterior (A), dorsal (B), right (C) and left (D) lateral views presented. Features are overlaid on a neonate-specific atlas image.

to the median value of continuous variables (*e.g.*, motion parameters) failed to differentiate groups accurately. Comparable analyses using only data from preterm-born infants also failed to differentiate groups. These results suggest the investigated variables did not drive group differentiation. In addition, due to differences in PMA at scan between the term and preterm groups, a SVM classifier was created using only data from the oldest 25 preterm subjects and youngest 25 term subjects (mean preterm scan age 39 ± 1 weeks and mean term scan age 38 ± 1 weeks; *n.b.*, preterm > term in contrast to the analysis using all subjects). This analysis also accurately classified term and preterm subjects (accuracy 82%, sensitivity 88%, specificity 76%, $p < 0.00001$).

Finally, to further mitigate any potential confounding effects present due to subject motion during data acquisition, SVM analysis was also performed using only the 35 subjects from each group with 5 min of data passing more stringent motion criteria than those detailed above ("super scrubbing"; frame exclusion criteria framewise displacement ≥0.25 mm or DVARS ≥0.3%). Classification results were again similar to those obtained using all subjects, with 108 consensus inter- and intra-hemispheric features within and between RSNs important for group categorization (accuracy 80%, sensitivity 83%, specificity 77%, $p < 0.00001$; see also Supplemental Fig. 2).

Table 2
Binary SVM results for subjects categorized by demographic, clinical and technical variables.

Variable	Group size	Accuracy (%)	Sensitivity (%)	Specificity (%)	p value
All subjects	50	84	90	78	<0.00001
Sex — male	26	83	88	78	<0.00001
Race — AA	23	76	83	70	0.0002
Scan PMA	25	82	88	76	<0.00001
Atlas scale — term	25	56	60	52	0.08
Atlas scale — preterm	25	48	52	44	0.11
RMS — term	25	52	52	52	0.11
RMS — preterm	25	54	60	48	0.08
Super scrubbing	35	80	83	77	<0.00001

SVR birth gestational age prediction

Using GA at birth as the training measure, SVR was used to make quantitative predictions of GA at birth in individual infants based upon the single rs-fMRI data sets collected at term equivalent PMA. In this analysis, 118 consensus features were identified, with location and weighting comparable to results obtained in the SVM group analysis (Supplemental Figs. 3 and 4). Again, connections within and between networks located throughout the brain were typically greater in term-born infants. As expected, predicted birth GA values were typically greater in term (36 ± 4 weeks) than preterm (30 ± 4 weeks) infants based upon individual data sets, differentiating the two infant groups ($p < 0.00001$). Use of a linear model to fit these data illustrated that higher birth GA led to prediction of greater connectivity measures at term equivalent ($r = 0.61$, $p < 0.00001$) (Fig. 4). The model performed comparably for both infant groups. Differences in the absolute value between the actual GA at birth and the SVR-estimated GA at birth were calculated for each infant and averaged across groups. For both groups, the mean difference between actual and SVR-estimated GA measures was 4 weeks ($p = 0.98$).

Discussion

Summary of findings

Binary SVMs applied to rs-fMRI data reliably categorized term-born and preterm-born infants at term equivalent PMA. Inter- and intra-hemispheric functional connections throughout the brain that were important for group categorization were typically stronger in infants born at term. Model accuracy was not driven by group differences in sex, race, PMA at scan, atlas scaling or motion parameters. Extension to SVR enabled quantitative predictions of GA at birth in individual subjects from both groups that were correlated with actual GA at birth. These findings illustrate brain-wide alterations of functional cerebral development for preterm-born infants at both the group and individual level by term equivalent, extending prior reports in this population (Damaraju et al., 2010; Smyser et al., 2010, 2016). Importantly, the ability of SVR to predict GA at birth indicates that this approach is sensitive to the extent of disruption of brain development associated with the degree of prematurity at birth. Thus, this approach has the potential to be used to determine a brain maturity index at term equivalent for individual infants, which may assist in presymptomatic prediction of later neurodevelopmental outcomes.

Relation to prior multivariate pattern analysis (MVPA) studies

The power of MVPA lies in its capacity to incorporate large amounts of information to develop classification models. When applied to neuroimaging data, MVPA leverages information extracted from regions across the brain, removing artificial restrictions to specific connections, regions or networks common in prior functional neuroimaging investigations (Norman et al., 2006; Pereira et al., 2009; Pruett et al., 2015; Smola, 2004). This brain-wide approach is resistant to overfitting while enabling less robust, spatially distributed data to cumulatively contribute to results (*i.e.*, many connections weakly associated with group classification collectively create a powerful model) (Pruett et al., 2015; Satterthwaite et al., 2014).

These inherent attributes have recently led to rapid expansion in the use of machine-learning classifiers to analyze neuroimaging data, and the methods have been applied to investigate changes associated with normal development, aging and clinical diagnoses such as autism, Alzheimer's disease, schizophrenia, addiction and obsessive–compulsive disorder (Brown et al., 2012; Ecker et al., 2010; Erus et al., 2014; Fair et al., 2012; Franke et al., 2012, 2010; Li et al., 2014; Magnin et al., 2009; Pruett et al., 2015; Satterthwaite et al., 2014). Each investigation has reported a strong ability to differentiate clinical populations from

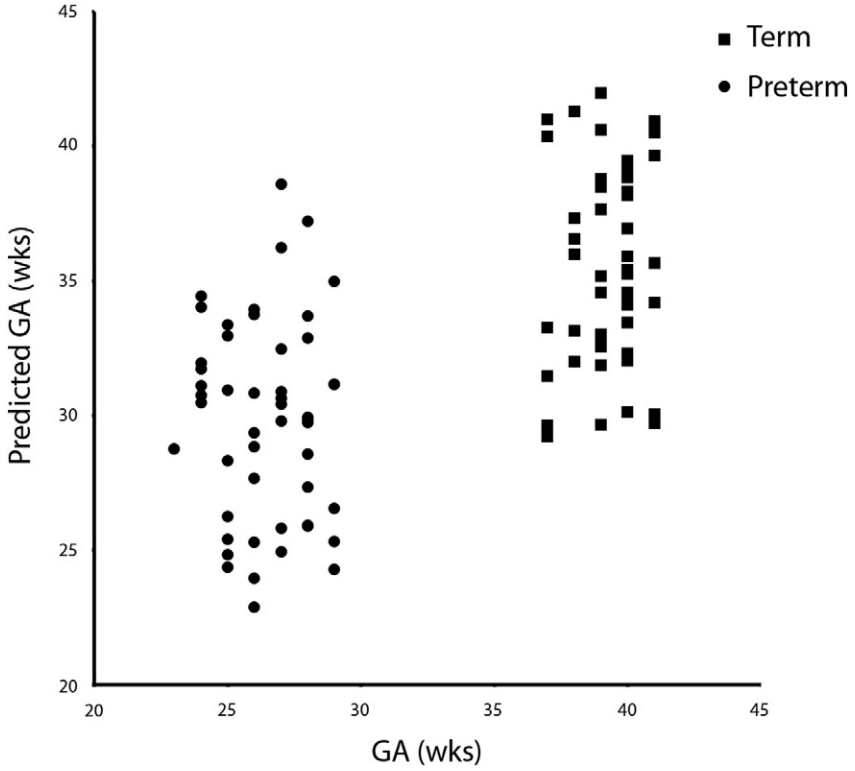

Fig. 4. Support vector regression results depicting actual (x-axis) *versus* predicted (y-axis) gestational age (GA) for term-born and preterm-born infants determined using individual term equivalent rs-fMRI data sets (preterm-born infants = circles, term-born infants = squares). Note the delineation in predicted gestational age values between infants within each group, reflecting differences in functional connectivity measures between term and preterm subjects scanned at comparable postmenstrual age.

control subjects (typically >80% accuracy with some rates as high as 95%) using structural, diffusion, task-based or resting state MRI data. Model accuracy is improved when combining data obtained across complementary imaging modalities (Brown et al., 2012; Erus et al., 2014). The approach is well-suited to the study of increasingly diverse subject groups, ranging from infant (Pruett et al., 2015) to geriatric populations (Vergun et al., 2013). In addition, the ability to extract information regarding the relative importance of both connections and nodes *via* feature weights highlights changes within specific regions and/or networks attributable to age or disease. Extension of this methodology to SVR has enabled development of models that can predict individual age and performance (Erus et al., 2014; Vergun et al., 2013). The heterogeneity across these studies illustrates the power and adaptability of this technique.

Relation to prior infant rs-fMRI investigations

Our investigation capitalizes upon the benefits of MVPA to extend prior neonatal rs-fMRI investigations of infants (Doria et al., 2010; Fransson et al., 2009, 2007; Gao et al., 2014; Lin et al., 2008; Smyser et al., 2010, 2016). Recently, intrinsic fMRI activity was found to be quantitatively reduced and have decreased complexity in preterm-born infants (Smyser et al., 2016). Our results validate and expand upon these findings at the group level and extend them to the individual subject level, with the consistency and pattern of feature weights illustrating the scope and scale of the effects of prematurity. Importantly, our SVM models retained sufficient power to differentiate term-born and preterm-born neonates despite targeted removal of ROIs with functional connections of the greatest relative classification power. This suggests that differences in functional connectivity between these groups are not dependent upon small numbers of regions or features, though some may carry greater importance in distinguishing neonatal populations.

Consensus features for both SVM and SVR were widely distributed, incorporating functionally defined ROIs from the default mode, cingulo-opercular, somatomotor and dorsal attention networks (Cohen et al., 2008; Power et al., 2011). Summing weights and performing RSN-specific analyses revealed that both early maturing motor and sensory networks and higher-order RSNs, such as the default mode, cingulo-opercular, dorsal attention and salience networks, contributed to successful categorization. These higher-order RSNs have been shown to develop more slowly than motor and sensory networks during this developmental period, following known rates of cortical maturation and shaped by the complex interplay of intrinsic activity and external stimuli (Ferradal et al., 2015; Gao et al., 2014; Smyser et al., 2016). The patterns of decreased correlation strength demonstrated in preterm-born infants suggest that functional connections throughout the brain are disturbed by the time of discharge from the NICU and occur even without significant brain injury. A growing body of evidence suggests that the immature brain may be susceptible to deleterious deprivation (*e.g.*, inadequate nutrition, minimal auditory exposure) and/or noxious exposures (*e.g.*, noxious stimuli, medications) inherent to the NICU environment (Brummelte et al., 2012; Caskey et al., 2014; Dabydeen et al., 2008; Ferguson et al., 2012; Pineda et al., 2014; Smith et al., 2011).

Neurodevelopmental implications

Preterm children face a range of neurodevelopmental and neurobehavioral challenges, with those born earliest facing disproportionate risk (Marlow et al., 2005; Saigal and Doyle, 2008; Woodward et al., 2009). Prior investigations have characterized the alterations in cerebral gray and white matter development associated with preterm birth using conventional MRI (Inder et al., 2005; Miller et al., 2005; Woodward et al., 2006). However, comparable studies employing rs-fMRI have been limited in number and scale, with few studies focused upon infancy (Damaraju et al., 2010; Doria et al., 2010; Fransson et al.,

2007; Smyser et al., 2010). These investigations have demonstrated group differences in quantitative comparisons of term-born and preterm-born infants. The etiology of these differences remains unknown, though it is suspected that an amalgam of common NICU exposures contributes individually or cumulatively to these alterations in rs-fMRI measures (Ball et al., 2010; Brummelte et al., 2012; Chau et al., 2012; Ferguson et al., 2012; Smith et al., 2011). Importantly, there is evidence that intrinsic cortical and subcortical neuronal activity is critical for early brain development (Katz and Crowley, 2002), and that affected RSNs play critical roles in cognitive, motor and language function in adults (Fox and Greicius, 2010). Subsequently, these connectivity differences may correlate with the neurodevelopmental deficits common in preterm-born infants (Burton et al., 2009; Posner et al., 2014; Redcay et al., 2013).

It is important to note that SVM only successfully differentiated infants using birth GA as the variable of interest. Targeted investigation revealed no differences in this same cohort of infants separated using sex, race, PMA at scan, atlas scaling and motion parameters, some of which are important determinants of neurodevelopmental outcomes among prematurely-born infants. Therefore, in this model, this observation places degree of prematurity as the most powerful variable in determining functional brain network development among very preterm infants without significant cerebral injury, just as it is one of the most powerful variables in determining long-term neurodevelopmental outcomes (Marlow et al., 2005). Thus, our findings suggest that aberrant functional connectivity may be a critical factor in mediating downstream neurodevelopmental disability.

The finding that SVR analysis of rs-fMRI data at term equivalent can be used to identify degree of prematurity (GA at birth) provides proof of principle that rs-fMRI data may play a role predicting neurodevelopmental outcome. GA at birth was used as an indicator of the degree of disruption of brain development present at term equivalent PMA for this study, assuming that, on average, greater degrees of prematurity are associated with greater degrees of disruption of brain development. The capacity of SVR to estimate birth GA raises the possibility of developing a "maturity index", such as an index based on the SVR-estimated GA at birth obtained at term equivalent PMA. If such a measure proves to be associated with neurodevelopmental outcome, then quantitative imaging measures obtained using this approach could serve as a method for early identification of infants at highest risk for subsequent neurodevelopmental disability. It also has the potential to provide biomarkers for future NICU intervention trials of neuroprotective strategies or to permit timely intervention designed to maximize an individual's neurodevelopmental outcome. In addition, it is worth noting that SVR methods are not restricted to analysis of rs-fMRI data, but provide a framework for translating results across multiple modalities. Thus, this approach can be extended to incorporate complementary data types (*e.g.*, electroencephalogram, physiological monitoring, serum metabolites), further improving model accuracy (Mueller et al., 2013; Temko et al., 2011).

While this representative application of SVR in this population demonstrates its potential, it also provides interesting results. For example, the GA estimates from the SVR approach were within 4 weeks of the actual values on average, with estimated values both larger and smaller than actual values. Thus, the majority of preterm infants were accurately estimated to be born prematurely (and term infants were correspondingly estimated to be born at or near term). In addition, estimated measures show overlap between the term-born and preterm-born populations (Fig. 4). It is unknown whether this scatter/overlap in GA estimates is due to biological variability or related to methodological issues such as noise in the measurements. Because a subpopulation of preterm-born infants have typical neurodevelopmental outcomes, it is conceivable that the scatter is real, with some of the preterm-born infants displaying network architecture that would be appropriate for the term-born range (*i.e.*, $\geq$36 weeks). This is particularly true in this study, as we excluded any infant with moderate or severe cerebral abnormality on conventional MRI studies, which remains among the strongest current predictors of outcome (Hintz et al., 2015; Woodward et al., 2006). Conversely, the term infants with low birth GA estimates (*i.e.*, $\leq$32 weeks) may be at greater than anticipated risk of adverse neurodevelopmental outcomes. Importantly, the infants from both term and preterm cohorts with overlapping GA estimates did not demonstrate differences in clinical variables either between (*i.e.*, overlapping preterm *versus* overlapping term) or within groups (*i.e.*, overlapping preterm *versus* non-overlapping preterm). Thus, prediction of birth GA may be approximate to assessment of brain maturity, identifying those infants who would benefit most from additional close monitoring of neurodevelopmental performance and/or neurodevelopmental intervention during infancy and childhood (*i.e.*, the majority of preterm infants and a targeted subset of term infants in this sample).

While the correlation coefficient for actual *versus* predicted GA was relatively modest ($r = 0.61$), this value is affected by three factors. First, the methodology, by definition, brings values closer to the mean; as such, it is anticipated that term-born infants will have lower predicted than actual GA values and preterm-born infants higher predicted than actual GA values, both of which affect the correlation coefficient. Second, the clinical estimates of GA used are generally considered to be accurate within two weeks (and approximately one third of our study population had one or fewer prenatal visits). Third, variability in individual brain networks, as noted above, would also serve to increase apparent scatter in the GA estimates and reduce the correlation coefficient. When considering the magnitude of the correlation coefficient in the context of these methodological and clinical considerations, and the high level of statistical significance for the model with a (relatively) modest sample size, we contend that the result indicates that this approach may be useful for predicting outcome.

Caveats and limitations

Because of rigorous data quality criteria pertaining to motion, this investigation included a total of 100 infants, with 50 subjects in each group. This sample size is relatively modest in comparison to SVM investigations in older populations, but large in relation to previous neonatal investigations (Doria et al., 2010; Fransson et al., 2009, 2007; Lin et al., 2008; Smyser et al., 2016). In addition, potential effects of using ROIs defined in older populations are difficult to evaluate, though ROIs located outside of gray matter were identified using quantitative and qualitative approaches and excluded from subsequent analyses. Further, though atlas registration was comparable across groups, this may not encapsulate subtle anatomic differences between preterm and term subjects. As a result, it is difficult to determine if these potential registration or image contrast differences may contribute to the high model accuracy due to the sensitivity of SVM.

Finally, optimal methods for rs-fMRI data acquisition and preprocessing for this population have not yet been rigorously defined. These include the optimal spatial resolution and echo times. Further still, the effects of infant state during data acquisition, such as awake/asleep and sleep stage, on rs-fMRI results have yet to be carefully explored. For this study, we selected approaches that have been employed by our group and others to successfully study infants across multiple prior investigations, but much work remains to be completed in this area.

Conclusions

We employed multivariate pattern classification methods to analyze neonatal rs-fMRI data and demonstrated differences between term-born and preterm-born infants scanned at term equivalent PMA. The network alterations detected were not specific to a particular brain region, as binary SVMs identified widespread inter- and intra-hemispheric connections within and between RSNs important for group categorization. These features were typically stronger (*i.e.*,

correlation coefficients were greater) in infants born at term and were not dependent upon sex, race, PMA at scan, atlas scaling and motion parameter differences. Further, the use of SVR enabled quantitative predictions regarding birth GA in individual subjects, indicating that these brain-wide, computationally intensive approaches may allow development of models for defining indices of brain maturation at the time of discharge from the NICU that enable presymptomatic prediction of the risk for subsequent neurodevelopmental adversity.

Supplementary data to this article can be found online at http://dx.doi.org/10.1016/j.neuroimage.2016.05.029.

Conflicts of interest

The authors report no conflicts of interest.

Acknowledgments

The authors thank Jeanette K. Kenley and Joshua S. Shimony for assistance with data analysis; Alison G. Cahill and Amit M. Mathur for providing data; and Adam Eggebrecht, Siddharth Jain and Lillian Matthews for useful comments on the manuscript.

This work was supported by the National Institutes of Health [grant numbers K02 NS089852 to C.D.S., UL1 TR000448 to C.D.S, K12 HD076224 to N.U.F.D., K23 NS088590 to N.U.F.D., K23 MH105179 to C.E.R., R01 HD05709801 to T.E.I. and J.J.N., P30 NS048056 to A.Z.S., P30 HD062171 and R01 HD061619]; Child Neurology Foundation [to C.D.S. and N.U.F.D.]; Cerebral Palsy International Research Foundation [to C.D.S.]; The Dana Foundation [to C.D.S.]; and the Barnes-Jewish Hospital Foundation. Research reported in this publication was also supported by the Eunice Kennedy Shriver National Institute of Child Health & Human Development of the National Institutes of Health under Award Number U54HD087011 to the Intellectual and Developmental Disabilities Research Center at Washington University. The National Institutes of Health and other funders had no role in study design, data collection and analysis, decision to publish or preparation of the manuscript and the content is solely the responsibility of the authors.

References

Ball, G., Counsell, S.J., Anjari, M., Merchant, N., Arichi, T., Doria, V., Rutherford, M.A., Edwards, A.D., Rueckert, D., Boardman, J.P., 2010. An optimised tract-based spatial statistics protocol for neonates: applications to prematurity and chronic lung disease. NeuroImage 53, 94–102.

Ben-Hur, A., Ong, C.S., Sonnenburg, S., Scholkopf, B., Ratsch, G., 2008. Support vector machines and kernels for computational biology. PLoS Comput. Biol. 4, e1000173.

Brown, T.T., Kuperman, J.M., Chung, Y., Erhart, M., McCabe, C., Hagler Jr., D.J., Venkatraman, V.K., Akshoomoff, N., Amaral, D.G., Bloss, C.S., Casey, B.J., Chang, L., Ernst, T.M., Frazier, J.A., Gruen, J.R., Kaufmann, W.E., Kenet, T., Kennedy, D.N., Murray, S.S., Sowell, E.R., Jernigan, T.L., Dale, A.M., 2012. Neuroanatomical assessment of biological maturity. Curr. Biol. 22, 1693–1698.

Brummelte, S., Grunau, R.E., Chau, V., Poskitt, K.J., Brant, R., Vinall, J., Gover, A., Synnes, A.R., Miller, S.P., 2012. Procedural pain and brain development in premature newborns. Ann. Neurol. 71, 385–396.

Burton, H., Dixit, S., Litkowski, P., Wingert, J.R., 2009. Functional connectivity for somatosensory and motor cortex in spastic diplegia. Somatosens. Mot. Res. 26, 90–104.

Caskey, M., Stephens, B., Tucker, R., Vohr, B., 2014. Adult talk in the NICU with preterm infants and developmental outcomes. Pediatrics 133, e578–e584.

Chau, V., Brant, R., Poskitt, K.J., Tam, E.W., Synnes, A., Miller, S.P., 2012. Postnatal infection is associated with widespread abnormalities of brain development in premature newborns. Pediatr. Res. 71, 274–279.

Cohen, A.L., Fair, D.A., Dosenbach, N.U., Miezin, F.M., Dierker, D., Van Essen, D.C., Schlaggar, B.L., Petersen, S.E., 2008. Defining functional areas in individual human brains using resting functional connectivity MRI. NeuroImage 41, 45–57.

Dabydeen, L., Thomas, J.E., Aston, T.J., Hartley, H., Sinha, S.K., Eyre, J.A., 2008. High-energy and protein diet increases brain and corticospinal tract growth in term and preterm infants after perinatal brain injury. Pediatrics 121, 148–156.

Damaraju, E., Phillips, J.R., Lowe, J.R., Ohls, R., Calhoun, V.D., Caprihan, A., 2010. Resting-state functional connectivity differences in premature children. Front. Syst. Neurosci. 4.

Doria, V., Beckmann, C.F., Arichi, T., Merchant, N., Groppo, M., Turkheimer, F.E., Counsell, S.J., Murgasova, M., Aljabar, P., Nunes, R.G., Larkman, D.J., Rees, G., Edwards, A.D., 2010. Emergence of resting state networks in the preterm human brain. Proc. Natl. Acad. Sci. U. S. A. 107, 20015–20020.

Dosenbach, N.U., Nardos, B., Cohen, A.L., Fair, D.A., Power, J.D., Church, J.A., Nelson, S.M., Wig, G.S., Vogel, A.C., Lessov-Schlaggar, C.N., Barnes, K.A., Dubis, J.W., Feczko, E., Coalson, R.S., Pruett Jr., J.R., Barch, D.M., Petersen, S.E., Schlaggar, B.L., 2010. Prediction of individual brain maturity using fMRI. Science 329, 1358–1361.

Ecker, C., Rocha-Rego, V., Johnston, P., Mourao-Miranda, J., Marquand, A., Daly, E.M., Brammer, M.J., Murphy, C., Murphy, D.G., 2010. Investigating the predictive value of whole-brain structural MR scans in autism: a pattern classification approach. NeuroImage 49, 44–56.

Erus, G., Battapady, H., Satterthwaite, T.D., Hakonarson, H., Gur, R.E., Davatzikos, C., Gur, R.C., 2014. Imaging patterns of brain development and their relationship to cognition. Cereb. Cortex.

Fair, D.A., Nigg, J.T., Iyer, S., Bathula, D., Mills, K.L., Dosenbach, N.U., Schlaggar, B.L., Mennes, M., Gutman, D., Bangaru, S., Buitelaar, J.K., Dickstein, D.P., Di Martino, A., Kennedy, D.N., Kelly, C., Luna, B., Schweitzer, J.B., Velanova, K., Wang, Y.F., Mostofsky, S., Castellanos, F.X., Milham, M.P., 2012. Distinct neural signatures detected for ADHD subtypes after controlling for micro-movements in resting state functional connectivity MRI data. Front. Syst. Neurosci. 6, 80.

Ferguson, S.A., Ward, W.L., Paule, M.G., Hall, R.W., Anand, K.J., 2012. A pilot study of preemptive morphine analgesia in preterm neonates: effects on head circumference, social behavior, and response latencies in early childhood. Neurotoxicol. Teratol. 34, 47–55.

Ferradal, S.L., Liao, S.M., Eggebrecht, A.T., Shimony, J.S., Inder, T.E., Culver, J.P., Smyser, C.D., 2015. Functional imaging of the developing brain at the bedside using diffuse optical tomography. Cereb. Cortex.

Fox, M.D., Greicius, M., 2010. Clinical applications of resting state functional connectivity. Front. Syst. Neurosci. 4, 19.

Franke, K., Ziegler, G., Kloppel, S., Gaser, C., 2010. Estimating the age of healthy subjects from T1-weighted MRI scans using kernel methods: exploring the influence of various parameters. NeuroImage 50, 883–892.

Franke, K., Luders, E., May, A., Wilke, M., Gaser, C., 2012. Brain maturation: predicting individual BrainAGE in children and adolescents using structural MRI. NeuroImage 63, 1305–1312.

Fransson, P., Skiold, B., Horsch, S., Nordell, A., Blennow, M., Lagercrantz, H., Aden, U., 2007. Resting-state networks in the infant brain. Proc. Natl. Acad. Sci. U. S. A. 104, 15531–15536.

Fransson, P., Skiold, B., Engstrom, M., Hallberg, B., Mosskin, M., Aden, U., Lagercrantz, H., Blennow, M., 2009. Spontaneous brain activity in the newborn brain during natural sleep–an fMRI study in infants born at full term. Pediatr. Res. 66, 301–305.

Gao, W., Alcauter, S., Elton, A., Hernandez-Castillo, C.R., Smith, J.K., Ramirez, J., Lin, W., 2014. Functional network development during the first year: relative sequence and socioeconomic correlations. Cereb Cortex.

Gholipour, A., Kehtarnavaz, N., Gopinath, K., Briggs, R., Panahi, I., 2008. Average field map image template for Echo-planar image analysis. Conf. Proc. IEEE Eng. Med. Biol. Soc. 2008, 94–97.

Hintz, S.R., Barnes, P.D., Bulas, D., Slovis, T.L., Finer, N.N., Wrage, L.A., Das, A., Tyson, J.E., Stevenson, D.K., Carlo, W.A., Walsh, M.C., Laptook, A.R., Yoder, B.A., Van Meurs, K.P., Faix, R.G., Rich, W., Newman, N.S., Cheng, H., Heyne, R.J., Vohr, B.R., Acarregui, M.J., Vaucher, Y.E., Pappas, A., Peralta-Carcelen, M., Wilson-Costello, D.E., Evans, P.W., Goldstein, R.F., Myers, G.J., Poindexter, B.B., McGowan, E.C., Adams-Chapman, I., Fuller, J., Higgins, R.D., 2015. Neuroimaging and neurodevelopmental outcome in extremely preterm infants. Pediatrics 135, e32–e42.

Inder, T.E., Warfield, S.K., Wang, H., Huppi, P.S., Volpe, J.J., 2005. Abnormal cerebral structure is present at term in premature infants. Pediatrics 115, 286–294.

Jenkins, G., Watts, D., 1968. Spectral Analysis and Its Applications. Holden-Day, San Francisco.

Jenkinson, M., Beckmann, C.F., Behrens, T.E., Woolrich, M.W., Smith, S.M., 2012. Fsl. Neuroimage 62, 782–790.

Katz, L.C., Crowley, J.C., 2002. Development of cortical circuits: lessons from ocular dominance columns. Nat. Rev. Neurosci. 3, 34–42.

Kohavi, R., 1995. A study of cross-validation and bootstrap for accuracy estimation and model selection. International Joint Conference on Artificial Intelligence (JCAI). Morgan Kaufmann, Montreal, Canada.

Li, F., Huang, X., Tang, W., Yang, Y., Li, B., Kemp, G.J., Mechelli, A., Gong, Q., 2014. Multivariate pattern analysis of DTI reveals differential white matter in individuals with obsessive–compulsive disorder. Hum. Brain Mapp. 35, 2643–2651.

Lin, W., Zhu, Q., Gao, W., Chen, Y., Toh, C.H., Styner, M., Gerig, G., Smith, J.K., Biswal, B., Gilmore, J.H., 2008. Functional connectivity MR imaging reveals cortical functional connectivity in the developing brain. AJNR Am. J. Neuroradiol. 29, 1883–1889.

Magnin, B., Mesrob, L., Kinkingnehun, S., Pelegrini-Issac, M., Colliot, O., Sarazin, M., Dubois, B., Lehericy, S., Benali, H., 2009. Support vector machine-based classification of Alzheimer's disease from whole-brain anatomical MRI. Neuroradiology 51, 73–83.

Marlow, N., Wolke, D., Bracewell, M.A., Samara, M., 2005. Neurologic and developmental disability at six years of age after extremely preterm birth. N. Engl. J. Med. 352, 9–19.

Mathur, A.M., Neil, J.J., McKinstry, R.C., Inder, T.E., 2008. Transport, monitoring, and successful brain MR imaging in unsedated neonates. Pediatr. Radiol. 38, 260–264.

Meier, T.B., Desphande, A.S., Vergun, S., Nair, V.A., Song, J., Biswal, B.B., Meyerand, M.E., Birn, R.M., Prabhakaran, V., 2012. Support vector machine classification and characterization of age-related reorganization of functional brain networks. NeuroImage 60, 601–613.

Miller, S.P., Ferriero, D.M., Leonard, C., Piecuch, R., Glidden, D.V., Partridge, J.C., Perez, M., Mukherjee, P., Vigneron, D.B., Barkovich, A.J., 2005. Early brain injury in premature newborns detected with magnetic resonance imaging is associated with adverse early neurodevelopmental outcome. J. Pediatr. 147, 609–616.

Mueller, M., Almeida, J.S., Stanislaus, R., Wagner, C.L., 2013. Can machine learning methods predict extubation outcome in premature infants as well as clinicians? J. Neonatal. Biol. 2.

Norman, K.A., Polyn, S.M., Detre, G.J., Haxby, J.V., 2006. Beyond mind-reading: multi-voxel pattern analysis of fMRI data. Trends Cogn. Sci. 10, 424–430.
Pariyadath, V., Stein, E.A., Ross, T.J., 2014. Machine learning classification of resting state functional connectivity predicts smoking status. Front. Hum. Neurosci. 8, 425.
Pereira, F., Mitchell, T., Botvinick, M., 2009. Machine learning classifiers and fMRI: a tutorial overview. NeuroImage 45, S199–S209.
Pineda, R.G., Neil, J., Dierker, D., Smyser, C.D., Wallendorf, M., Kidokoro, H., Reynolds, L.C., Walker, S., Rogers, C., Mathur, A.M., Van Essen, D.C., Inder, T., 2014. Alterations in brain structure and neurodevelopmental outcome in preterm infants hospitalized in different neonatal intensive care unit environments. J. Pediatr. 164, 52–60, e52.
Posner, J., Park, C., Wang, Z., 2014. Connecting the dots: a review of resting connectivity MRI studies in attention-deficit/hyperactivity disorder. Neuropsychol. Rev. 24, 3–15.
Power, J.D., Cohen, A.L., Nelson, S.M., Wig, G.S., Barnes, K.A., Church, J.A., Vogel, A.C., Laumann, T.O., Miezin, F.M., Schlaggar, B.L., Petersen, S.E., 2011. Functional network organization of the human brain. Neuron 72, 665–678.
Power, J.D., Mitra, A., Laumann, T.O., Snyder, A.Z., Schlaggar, B.L., Petersen, S.E., 2014. Methods to detect, characterize, and remove motion artifact in resting state fMRI. NeuroImage 84, 320–341.
Power, J.D., Schlaggar, B.L., Petersen, S.E., 2015. Recent progress and outstanding issues in motion correction in resting state fMRI. NeuroImage 105, 536–551.
Pruett Jr., J.R., Kandala, S., Hoertel, S., Snyder, A.Z., Elison, J.T., Nishino, T., Feczko, E., Dosenbach, N.U., Nardos, B., Power, J.D., Adeyemo, B., Botteron, K.N., McKinstry, R.C., Evans, A.C., Hazlett, H.C., Dager, S.R., Paterson, S., Schultz, R.T., Collins, D.L., Fonov, V.S., Styner, M., Gerig, G., Das, S., Kostopoulos, P., Constantino, J.N., Estes, A.M., Petersen, S.E., Schlaggar, B.L., Piven, J., 2015. Accurate age classification of 6 and 12 month-old infants based on resting-state functional connectivity magnetic resonance imaging data. Dev. Cogn. Neurosci. 12, 123–133.
Redcay, E., Moran, J.M., Mavros, P.L., Tager-Flusberg, H., Gabrieli, J.D., Whitfield-Gabrieli, S., 2013. Intrinsic functional network organization in high-functioning adolescents with autism spectrum disorder. Front. Hum. Neurosci. 7, 573.
Robinson, E.C., Hammers, A., Ericsson, A., Edwards, A.D., Rueckert, D., 2010. Identifying population differences in whole-brain structural networks: a machine learning approach. NeuroImage 50, 910–919.
Rosa, M.J., Portugal, L., Hahn, T., Fallgatter, A.J., Garrido, M.I., Shawe-Taylor, J., Mourao-Miranda, J., 2015. Sparse network-based models for patient classification using fMRI. NeuroImage 105, 493–506.
Saigal, S., Doyle, L.W., 2008. An overview of mortality and sequelae of preterm birth from infancy to adulthood. Lancet 371, 261–269.
Satterthwaite, T.D., Wolf, D.H., Roalf, D.R., Ruparel, K., Erus, G., Vandekar, S., Gennatas, E.D., Elliott, M.A., Smith, A., Hakonarson, H., Verma, R., Davatzikos, C., Gur, R.E., Gur, R.C., 2014. Linked sex differences in cognition and functional connectivity in youth. Cereb Cortex.
Scholkopf, B., Smola, A.J., 2002. Learning With Kernels: Support Vector Machines, Regularization, Optimization and Beyond. MIT Press, Cambridge, MA.
Shen, H., Wang, L., Liu, Y., Hu, D., 2010. Discriminative analysis of resting-state functional connectivity patterns of schizophrenia using low dimensional embedding of fMRI. NeuroImage 49, 3110–3121.
Smith, G.C., Gutovich, J., Smyser, C., Pineda, R., Newnham, C., Tjoeng, T.H., Vavasseur, C., Wallendorf, M., Neil, J., Inder, T., 2011. Neonatal intensive care unit stress is associated with brain development in preterm infants. Ann. Neurol. 70, 541–549.
Smola, A.a.S.B., 2004. A tutorial on support vector regression. Stat. Comput. 14, 199–222.
Smyser, C.D., Inder, T.E., Shimony, J.S., Hill, J.E., Degnan, A.J., Snyder, A.Z., Neil, J.J., 2010. Longitudinal analysis of neural network development in preterm infants. Cereb. Cortex 20, 2852–2862.
Smyser, C.D., Snyder, A.Z., Shimony, J.S., Mitra, A., Inder, T.E., Neil, J.J., 2016. Resting-state network complexity and magnitude are reduced in prematurely born infants. Cereb Cortex 26, 322–333.
Temko, A., Thomas, E., Marnane, W., Lightbody, G., Boylan, G., 2011. EEG-based neonatal seizure detection with support vector machines. Clin. Neurophysiol. 122, 464–473.
Van Essen, D.C., Drury, H.A., Dickson, J., Harwell, J., Hanlon, D., Anderson, C.H., 2001. An integrated software suite for surface-based analyses of cerebral cortex. J. Am. Med. Inform. Assoc. 8, 443–459.
Vergun, S., Deshpande, A.S., Meier, T.B., Song, J., Tudorascu, D.L., Nair, V.A., Singh, V., Biswal, B.B., Meyerand, M.E., Birn, R.M., Prabhakaran, V., 2013. Characterizing functional connectivity differences in aging adults using machine learning on resting state fMRI data. Front. Comput. Neurosci. 7, 38.
Woodward, L.J., Anderson, P.J., Austin, N.C., Howard, K., Inder, T.E., 2006. Neonatal MRI to predict neurodevelopmental outcomes in preterm infants. N. Engl. J. Med. 355, 685–694.
Woodward, L.J., Moor, S., Hood, K.M., Champion, P.R., Foster-Cohen, S., Inder, T.E., Austin, N.C., 2009. Very preterm children show impairments across multiple neurodevelopmental domains by age 4 years. Arch. Dis. Child. Fetal Neonatal Ed. 94, F339–F344.